

## Tin-induced reconstructions of the Si(100) surface

A. A. Baski and C. F. Quate

*Department of Applied Physics, Stanford University, Stanford, California 94305*

J. Nogami

*Department of Physics, University of Wisconsin–Milwaukee, Milwaukee, Wisconsin 53201  
and Laboratory for Surface Studies, University of Wisconsin–Milwaukee, Milwaukee, Wisconsin 53201*

(Received 22 April 1991; revised manuscript received 31 July 1991)

The behavior of tin on the Si(100)  $2 \times 1$  surface has been studied using scanning tunneling microscopy. At room temperatures ( $T < 150^\circ\text{C}$ ), low coverages of Sn form dimer rows that are oriented perpendicular to the underlying Si dimer rows. As the coverage is increased, these rows pack into areas of two-dimensional order, forming small regions of  $2 \times 2$  near 0.5 monolayer (ML). For substrates annealed above  $500^\circ\text{C}$ , the following reconstructions are known to occur:  $c(4 \times 4)$  and  $2 \times 6$  below 0.5 ML,  $c(4 \times 8)$  for 0.5–1.0 ML, and  $1 \times 5$  for 1.0–1.5 ML. A number of structures are observed by scanning tunneling microscopy which are associated with these reconstructions. Both the  $c(4 \times 4)$  and  $2 \times 6$  phases consist of missing Si dimer trenches and stripelike structures which grow perpendicular to the Si dimer rows. As the coverage is increased, the  $c(4 \times 8)$  reconstruction occurs when chainlike structures, consisting of buckled Sn dimers, form on the surface between trenches. The  $1 \times 5$  phase then grows over this  $c(4 \times 8)$  layer and consists of bright features which are probably associated with Sn dimers. When more than 2 ML Sn is deposited and annealed, the surface undergoes a gross rearrangement and forms  $\{311\}$  facets.

### I. INTRODUCTION

The behavior of tin on the Si(100) surface demonstrates an abundance of surface structures and reconstructions. Although this system behaves very similarly to group-III-metal:Si(100) systems (e.g., Al, Ga, and In) near room temperature ( $T < 150^\circ\text{C}$ ), the annealed phases of Sn:Si(100) appear much more complicated and interesting. Our comprehensive study of this surface's coverage evolution ranges from 0.05 to 0.5 monolayer (ML) in the room-temperature regime and from 0.05 to over 2 ML in the annealed regime. A number of distinct structures are encountered on the Sn:Si(100) surface which are associated with each of its many reconstructions. The origin of these structures, as well as their ordering behavior with coverage, is investigated. Oftentimes, we observe the intermixing of such structures on a local scale, resulting in the loss of long-range order. Since scanning tunneling microscopy (STM) is able to probe surfaces on a local scale in real space, it is an ideal technique for exploring the complicated ordering behavior of the Sn:Si(100) system.

All sample preparation and measurements were performed in an ultrahigh-vacuum (UHV) system with facilities for sample heating, metal deposition, and characterization by low-energy electron diffraction (LEED) and STM.<sup>1,2</sup> The Si(100) samples were cut from commercial wafer stock and then chemically cleaned before introduction to vacuum. In UHV the wafers were flashed at  $1130\text{--}1150^\circ\text{C}$  for 2 min, held at  $1000^\circ\text{C}$  for 10 min, and then slowly cooled. The chamber pressure remained below  $2 \times 10^{-9}$  Torr during flashing. Tin was evaporated

from a heated tungsten basket onto substrates which were at or below  $150^\circ\text{C}$ . The deposition rate was calibrated by a quartz-crystal microbalance, and the coverage was controlled by timed exposure of the sample to the source. Typical deposition rates were between 0.5 and 2 ML/min. All coverages quoted in this work are the values calculated from the exposure time and deposition rate. The annealed Sn phases were obtained by subsequently heating the sample to temperatures between  $550$  and  $650^\circ\text{C}$  for 2–20 min. All STM imaging was done at room temperature.

### II. ROOM-TEMPERATURE BEHAVIOR ( $T \leq 150^\circ\text{C}$ )

LEED studies have not indicated an ordered reconstruction for nonannealed Sn depositions. Using STM, we have examined Sn growth on substrates near room temperature ( $T < 150^\circ\text{C}$ ) for 0.05–0.5 ML and observed local ordering of the surface. Figure 1 shows three STM topographs of the Si(100) surface with nominally (a) 0.1, (b) 0.15, and (c) 0.5 ML Sn deposited near room temperature. Figures 1(a) and 1(b) are empty-electronic-state images, taken while tunneling into the sample. Figure 1(c) is a filled-state image. Figure 1(a) shows a single-height atomic step running diagonally across the image and the rows of Si dimers which rotate by  $90^\circ$  across the step. The deposited Sn appears as bright rows aligned perpendicular to the underlying Si dimer rows. The bright rows are relatively long and only one unit cell wide ( $1a$ , where  $a = a_0/\sqrt{2} = 3.84 \text{ \AA}$ ), indicating strongly anisotropic growth. As the coverage is increased, the Sn rows pack

closer into small areas of two-dimensional order. At 0.15 ML [Fig. 1(b)] many of the rows are spaced apart by three unit cells, i.e.,  $3a$ . When the coverage is close to 0.5 ML [Fig. 1(c)], the Sn rows become less separated and form regions with a  $2a$  interrow spacing.

These “room-temperature” rows are also observed for a number of group-III metals (Al, Ga, and In) on Si(100).<sup>3–5</sup> In these systems a well-ordered  $2 \times 2$  reconstruction forms at 0.5 ML metal coverage. For the case of Sn, the rows do form small regions of  $2 \times 2$ , but these areas are separated by  $2a - 8a$  wide gaps that destroy any long-range order. As the coverage approaches 0.5 ML, these gaps are not filled in. Instead, bright features visible in Fig. 1(c) appear, arising from growth of the second layer. This behavior is in contrast to the group-III metals which form an ordered, complete  $2 \times 2$  layer at 0.5 ML and show second-layer growth above this coverage.<sup>3</sup>

These images also reveal a  $2a$  periodicity along the Sn rows. A comparison of the nominal Sn coverage to the observed row density shows that each row corresponds to one metal atom per Si  $1 \times 1$  unit cell. Since each metal row consists of maxima spaced  $2a$  apart, each of these maxima should be associated with two metal atoms. Previous work has suggested such a dimer structure for the  $2 \times 2$  reconstruction formed at 0.5 ML for the group-III metals Al, Ga, and In on Si(100).<sup>6–8</sup> A similar row

structure has also been observed for Si on Si(100) growth below  $350^\circ\text{C}$ .<sup>9</sup> In this case “diluted” Si dimer rows with a  $2a$  periodicity occur at lower growth temperatures, rather than the usual Si dimer rows with a  $1a$  periodicity.

Figures 2(a) and 2(b) show a dual-bias topograph taken tunneling into and out of the same sample area, thus reflecting empty [Fig. 2(a)] and filled [Fig. 2(b)] electronic states of the sample. In the filled-state image [Fig. 2(b)], Si dimer rows are located along the white lines running diagonally from the lower right-hand to upper left-hand corners. Bright Sn rows are oriented perpendicular to the Si dimer rows and have maxima (i.e., Sn dimers) located in the troughs between these underlying Si dimer rows. In the empty-state image [Fig. 2(a)], the Si dimer rows are located along the dark diagonal lines. Since the maxima along the Sn rows occur between the dark lines, they still lie in the troughs between Si dimer rows. Therefore, both the empty- and filled-state maxima of the Sn dimer rows are located between Si dimer rows.

Figures 2(c) and 2(d) show another dual-bias image that reflects the empty [Fig. 2(c)] and filled [Fig. 2(d)] states of the Sn:Si(100) sample. This image is a “curvature” image where each pixel represents the local curvature near that point in the original topographic data. This technique enhances the dimer structure of both the Si and Sn dimer rows, at the expense of increased line-by-line noise. The dangling bonds of the Si dimers are now visible. Once again, the empty- and filled-state maxima along the Sn row are located in the troughs between the underlying Si dimer rows. In this curvature image,

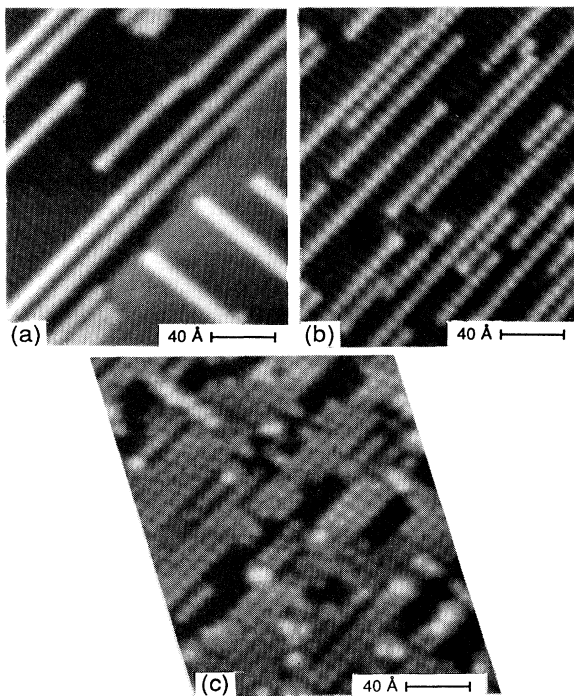


FIG. 1. Three images with (a) 0.1, (b) 0.15, and (c) 0.5 ML Sn deposited near room temperature. Both empty-electronic-state [(a) and (b)] and filled-state [(c)] images are shown. Bright Sn dimer rows are oriented perpendicular to the underlying Si dimer rows.

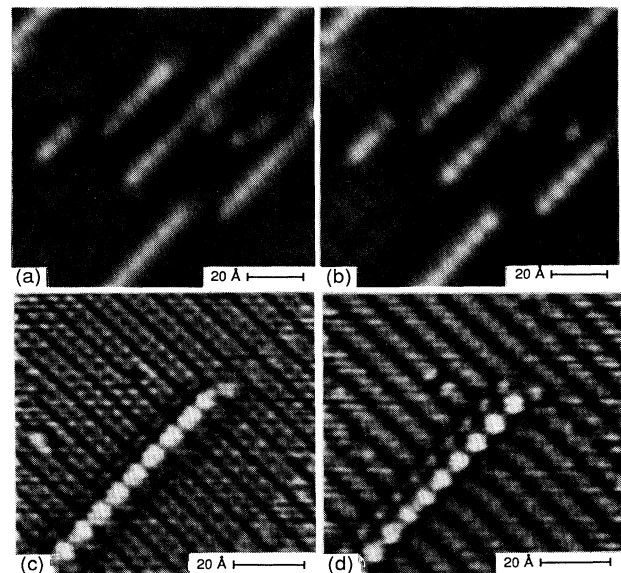


FIG. 2. (a), (b) Dual-bias topograph showing the (a) empty and (b) filled states of the Sn dimer rows. (c), (d) Dual-bias image showing the local curvature of the surface for the (c) empty and (d) filled states. The maxima along the Sn dimer rows are located in the troughs between the underlying Si dimer rows.

however, the Sn maxima appear slightly different in the two biases. In the filled-state image [Fig. 2(d)], each maximum is roughly circular. (There is a faint "double-tip" artifact in this bias which causes a shadow of the Sn row to appear just above it.) In the empty-state image [Fig. 2(c)], each maximum is elongated along the row and appears to consist of two overlapping features that resemble the dangling-bond structure of the Si dimers in the underlying layer. This image suggests that the maxima along the Sn row are Sn dimers which have the same orientation as the underlying Si dimers. Previous models of group-III metal rows on Si(100) have proposed the formation of dimers which are rotated  $90^\circ$  with respect to the Si dimer orientation.<sup>6,7,10</sup> If that were the case for Sn on Si(100), the elongation of the empty-state maxima would be perpendicular to the Sn-row direction. Although this image is not definitive, it certainly suggests that dimers may form where the dimer bond is parallel, not perpendicular, to the Sn-row direction.

Figure 3 illustrates the two possible orientations of the Sn dimers. Figure 3(a) has Sn dimers (solid circles) oriented with the dimer bond perpendicular to the underlying Si dimer bonds, as proposed previously by others. The Sn dimers in Fig. 3(b) are oriented with the dimer bond parallel to the Si dimer bonds, as suggested by Figs. 2(c) and 2(d). The parallel orientation might appear less feasible because of the large bond-angle distortions and the proximity of the Sn atoms to Si atoms in the second subsurface layer. It has been shown, however, that a similar adsorption site above second-layer Si atoms is energetically favorable for the case of adatoms on the Si(111) surface.<sup>11</sup> Consequently, the parallel configuration cannot be ruled out without a detailed calculation. This configuration also provides a natural explanation for the  $2a$  periodicity of the Sn rows. In the

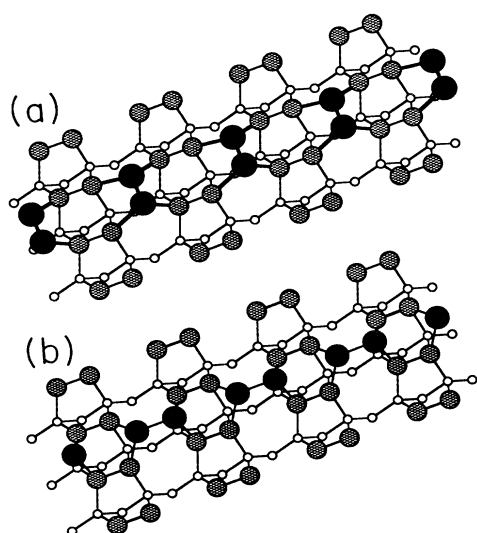


FIG. 3. Line drawing illustrating the (a) perpendicular and (b) parallel configurations for the Sn dimers in a single row (solid circles).

perpendicular configuration [Fig. 3(a)], one might argue that a  $1a$  periodicity should be possible via the insertion of additional dimers, as is observed for Si or As on Si(100). This  $1a$  periodicity is explicitly forbidden in the parallel-dimer configuration.

### III. ANNEALED BEHAVIOR UP TO 1.0 ML

LEED studies of the Sn:Si(100) surface indicate several annealed reconstructions between 0.1 and 1.5 ML.<sup>12</sup> For annealing treatments above  $500^\circ\text{C}$ , Sn induces four reconstructions as follows:  $c(4\times 4)$  for 0.2–0.375 ML,  $2\times 6$  for 0.375–0.5 ML,  $c(4\times 8)$  for 0.5–1.0 ML,  $1\times 5$  for 1.0–1.5 ML, and  $1\times 5$  plus streaks above 1.5 ML. These reconstructions are stable after cooling to room temperature. Our STM data show that the surface reconstructions up to 1 ML are constructed from different packings of structural subunits that will be referred to as trenches, stripes, and chains.

#### A. Trench and stripe structures

At coverages below 0.2 ML, trench structures form on the surface, which appear as dark lines oriented perpendicular to the Si dimer rows [Figs. 4(a) and 4(c)]. These trenches are spaced relatively far apart at low coverages (0.05 ML) and do not form very straight or long lines. As

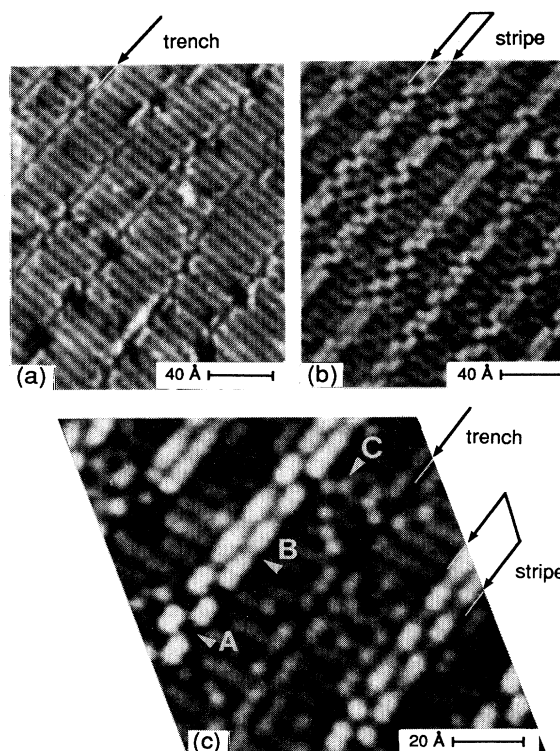


FIG. 4. Three filled-state images with nominally (a) 0.2, (b) 0.4, and (c) 0.4 ML Sn deposited and annealed. Both the trench and stripe structures are indicated.

the Sn coverage increases, they become more well defined and order into two-dimensional arrays with intertrench spacings of approximately  $8a-12a$  [Fig. 4(a) at 0.2 ML]. The existence of these well-ordered trenches at a relatively even spacing is also indicated by satellite dots in the LEED pattern. Figure 4(c) (0.4 ML) is a higher-magnification, filled-state image of one of these trench structures. The center of the trench appears dark in both the empty and filled electronic states, where the dark center line has a width slightly under one unit cell. This observation is consistent with the absence of one Si dimer every two unit cells along the length of the trench. The edges to either side of the trench appear significantly brighter in the empty states. This enhanced height difference is electronic in nature and could be caused by Sn substitution for the Si dimers situated along the edge of the trench. It should be noted that similar trench structures caused by missing Si dimers on clean Si(100) do not demonstrate this enhanced height difference. The simplest structural description of the trenches thus involves an arrangement of missing Si dimers and possible substitution of Sn for Si along the trench edges.

At coverages above 0.2 ML, another type of surface structure dominates. These structures appear in Figs. 4(b) and 4(c) as bright stripes oriented perpendicular to the Si dimer rows. Ordered arrays of these stripes usually occur, where the interstripe spacing decreases as the coverage increases. At a nominal coverage of 0.4 ML [Fig. 4(b)], the stripes have approximately an  $8a$  interstripe spacing (i.e., the centers of the stripes are eight unit cells apart). Using the unit-cell width defined by the resolved Si dimers in Fig. 4(c), the stripe structure is measured to be  $3a$  wide. This filled-state image shows stripes which have both well-ordered (arrow *A*) and disordered (arrow *B*) regions.

An interesting feature of Fig. 4(c) is the enhanced brightness and buckling of some of the dimers between the stripes and trenches (arrow *C*). These buckled dimers are caused by Sn substitution into the surface layer, as evidenced by an increase of the buckling with Sn coverage. When the surface consists primarily of these buckled dimers, chainlike structures form, which will be discussed in the next section.

We now examine the structure and dual-bias behavior of the stripe structure. Figures 5(a) and 5(b) show a dual-bias image of the empty [Fig. 5(a)] and filled [Fig. 5(b)] states of a surface near 0.5 ML. A single stripe is visible on the lower terrace, running parallel to, but clearly separated from, the step edge. Since this image is at a higher Sn coverage than the surface shown in Fig. 4(c), the areas surrounding the stripe have a chainlike appearance, which will be discussed in the following section. We focus here solely on the structure of the stripe itself. This stripe has a well-defined periodicity along its length that is representative of the ordered regions [Fig. 4(c), arrow *A*], rather than the disordered regions (arrow *B*) see a lower coverages. In general, as the Sn coverage is increased, the stripes appear to develop a more well-defined periodicity. The left and right sides of each stripe are symmetric in the empty states and  $180^\circ$  out of phase in the filled states. Figure 5(c) shows a cross-sectional trace

along the indicated left side of the stripe. The empty-state image (trace *A*) indicates a periodic corrugation with a  $2a$  periodicity. The filled-state image (trace *B*) shows double-peaked maxima which have a  $4a$  periodicity. The center of each double-peaked maximum in the filled states is located at the minimum of the periodic corrugation in the empty states. The registration of the empty- and filled-state maxima to the underlying  $1 \times 1$  lattice can also be obtained upon closer inspection of the filled-state image.

The registration and approximate spatial extent of the empty- and filled-state maxima of the stripe structure are diagrammed in Fig. 6. This figure contains one horizontal stripe which is three unit cells wide. Rows of unbuckled Si dimers (small, paired gray circles) are located to either side of the stripe. Both the dimers and stripe are situated one layer above the underlying  $1 \times 1$  lattice represented by the small open circles. The filled states of the stripe structure are represented by dark oblong features which consist of two closely spaced maxima. These oblongs are positioned antisymmetrically along the left and right sides of the stripe with a  $4a$  periodicity. The empty-state maxima are represented by gray circles that are symmetrically located along the left and right sides with a  $2a$  periodicity. The filled-state oblongs are centered between the empty-state circles. This arrangement of filled- and empty-state maxima naturally groups into subunits that each consist of an oblong filled state and two circular empty states. Coverage measurements of the stripe structure indicate that each subunit along the chain corresponds to approximately four Sn atoms.

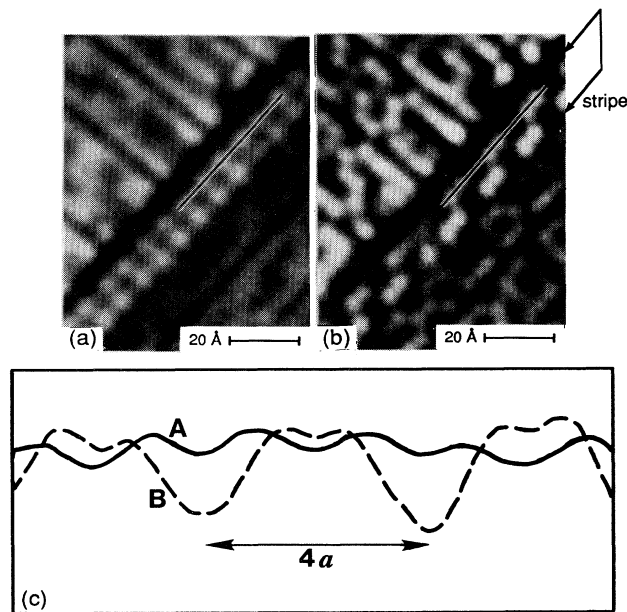


FIG. 5. Dual-bias image of a stripe showing the (a) empty and (b) filled states. The bottom line drawing [(c)] is a cross-sectional trace along the indicated left side of the stripe.

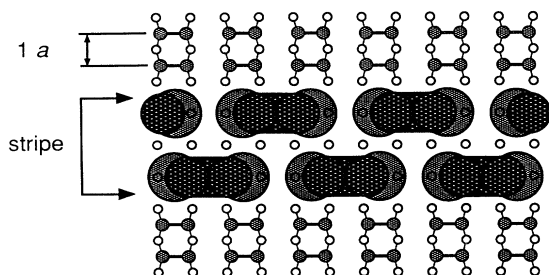


FIG. 6. Line drawing showing the filled-state (dark ovals) and empty-state (paired gray circles) maxima of the stripe structure.

Although Fig. 6 does not provide an atomic model, some limitations to a proposed structure are now evident. Any proposed model should incorporate approximately four atoms into each subunit along the stripe such that the empty and filled electronic states have the separation and registration as given in Fig. 6.

### B. Chain structures

As the coverage increases, another type of structure occurs which consists of trenches typically spaced  $4a$  or  $5a$  apart with chainlike rows located between them (Fig. 7, 0.8 ML). These linked structures are labeled "4-chains" ("5-chains"), where "4" ("5") refers to the chain width in  $1 \times 1$  unit cells. There is a  $4a$  periodicity along each of these chain structures. Near 1 ML, the 4-chains dominate the surface structure and only a few 5-chains occur. Since adjacent rows of 4-chains are  $180^\circ$  out of phase, the local surface order becomes  $c(4 \times 8)$ . This arrangement corresponds to the  $c(4 \times 8)$  reconstruction observed at 1 ML in previous LEED studies. Figure 8 is a

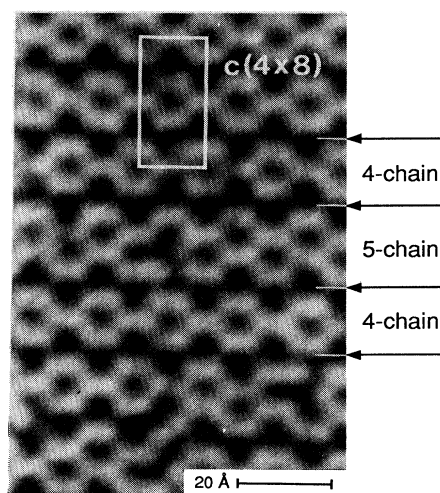


FIG. 7. Filled-state image (0.8 ML) showing the 4- and 5-chain structures. A  $c(4 \times 8)$  unit cell is indicated.

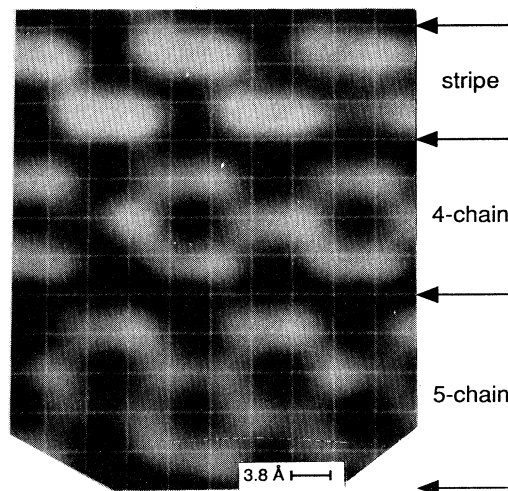


FIG. 8. Filled-state image with a superimposed  $1 \times 1$  unit-cell grid, which explicitly shows the widths of a stripe, 4-chain, and 5-chain.

high-magnification image of these chain structures with a  $1 \times 1$  unit-cell grid superimposed. From bottom to top a 5-chain ( $5a$  wide), 4-chain ( $4a$  wide), and a stripe structure ( $3a$  wide) can be seen.

A possible structural description for the chains involves the formation of buckled Sn-Sn dimers. The completion of the  $c(4 \times 8)$  phase at 1 ML indicates that all of the surface atoms of the chain structures are Sn. Using this assumption, Fig. 9 models the 4- and 5-chain struc-

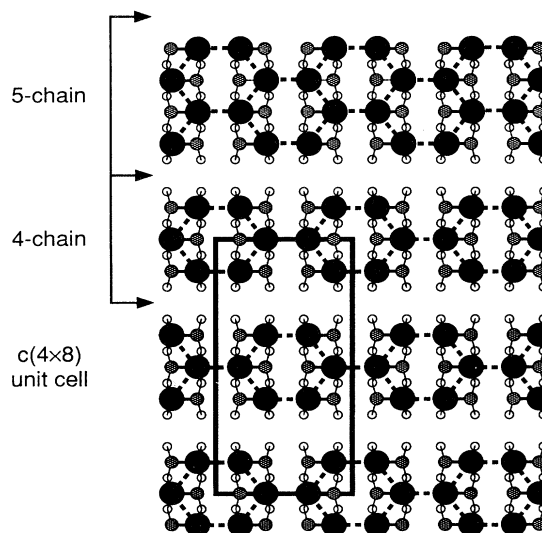


FIG. 9. Line drawing illustrating the proposed buckled Sn-Sn dimer model for the 4- and 5-chain structures. Each Sn dimer consists of a pair of gray and solid circles, where the solid circle represents the Sn atom buckled out of the surface plane that is visible in the filled-state images.

tures using buckled Sn-Sn surface dimers. Each dimer is shown as a pair of gray and solid circles. The larger solid circle represents the Sn atom buckled out of the surface plane that is visible in the filled-state images. The Sn dimers are situated one layer above the underlying  $1 \times 1$  lattice represented by small open circles. To form a 4-chain (5-chain), one Sn dimer is removed every four (five) unit cells along each of the Sn dimer rows (note that the Sn dimer rows are oriented perpendicular to the chain structures). The areas of missing Sn dimers correspond to the **dark trenches** observed between the chains in the images. The remaining Sn dimers are then alternatingly buckled along each dimer row to form the resulting chainlike structures. Although it is possible to construct the rows of chains to be in phase with each other, such ordering is never observed on the surface. This restriction results in the expected  $c(4 \times 8)$  reconstruction for the 4-chains near 1 ML.

Support for this simple model is drawn from comparisons between empty- and filled-state images of such buckled dimer structures. Figures 5(a) and 5(b) show a lower-coverage surface with a mixture of buckled and unbuckled surface atom dimers in the regions away from the previously discussed stripe structures. Since a mixture of Sn and Si atoms forms the surface dimers at this low coverage, the ordered chain structures have not yet been fully developed. Nevertheless, some segments of a 4-chain structure are visible, particularly in the area just below the stripe. The strong buckling in the filled states [Fig. 5(b)] is not very apparent in the empty states [Fig. 5(a)]. This behavior is the same as that observed for buckled dimers in STM images of either the Si(100) or Ge(100) surface. Dimers on these surfaces can appear buckled in the filled states, but look symmetric in the empty states.

The formation of the trenches between chains and the buckling of the Sn dimers are both manifestations of the stress induced by the Sn. As the proportion of Sn surface atoms increases, the fraction of buckled dimers increases and the spacing between trenches decreases. In the 1-ML  $c(4 \times 8)$  phase, trenches are spaced  $4a$  apart, which corresponds roughly to the 20% lattice mismatch between grey Sn and Si. The larger size of the Sn atoms induces compressive stress at the surface. Given that the clean Si(100) surface is under compressive stress normal to the dimer direction and under tensile stress along the dimers, the compressive stress from the Sn will be primarily normal to the dimers. The formation of trenches is a mechanism to relieve this stress. In addition, the buckling of the Sn dimers might also play a role in reducing the surface stress. For clean Si(100), the compressive surface stress normal to the dimers is over two times larger for unbuckled, versus buckled, dimers.<sup>13</sup>

### C. Complicated mixtures of stripe and chain structures

Up to this point, we have addressed the stripe and chain structures as separate entities in the coverage evolution of the surface. The stripe structures are more dominant at lower coverages, while the 4-chains cover

the surface near 1 ML. The surface can be quite complicated, however, in the coverage regime between approximately 0.4 and 0.8 ML. The stripe and chain structures oftentimes coexist and produce local regions with  $4 \times 14$ ,  $4 \times 6$ , and  $c(4 \times 4)$  order.

Previously, we found that near 0.4 ML the surface consisted of stripes with interstripe spacings between  $8a$  and  $12a$  [Fig. 4(b)]. The regions between the stripes consisted largely of unbuckled Si dimers, but the presence of buckled dimers did indicate the possibility of Sn dimer substitution. When an additional 0.2 ML is evaporated onto this surface and annealed, the surface resembles the filled-state image in Fig. 10 (0.6 ML). Stripes are prevalent on this particular surface, but a number of structures other than Si dimers occur in the regions between the stripes. In the upper half of the image, the interstripe spacing has decreased to  $7a$ . The stripes ( $3a$  wide) are now separated by 4-chains ( $4a$  wide). Given the  $4a$  periodicity along both the stripe and 4-chain structures, a  $4 \times 7$  unit cell results, with an alternation in phase of the chains giving an overall  $4 \times 14$  ordering. In the center of the image, a bright row of roundish features appears to grow one layer above the rest of the surface. We occasionally observe such features and believe that they are caused by excess Sn on the surface, which preferentially adsorbs on regions between stripes. In the lower half of the image, the interstripe spacing is  $6a$ , where the stripes ( $3a$  wide) are separated by 3-chains ( $3a$  wide). The 3-chain structures have not been previously addressed, but they are analogous to the 4- and 5-chain structures. This local region has  $4 \times 6$  ordering. Previous LEED studies have indicated a  $2 \times 6$  reconstruction near this coverage regime. Most likely, the  $4 \times$  periodicity is not evident in LEED because different regions of  $4 \times 6$  can be out of phase, as well as the  $4 \times$  periodicity along the stripe is not always well developed.

The complexity of the surface continues to increase when another 0.2 ML is evaporated onto the surface of Fig. 10 and annealed (Fig. 11, 0.8 ML). In the upper portion of the image, some stripes with a  $6a$  interstripe spac-

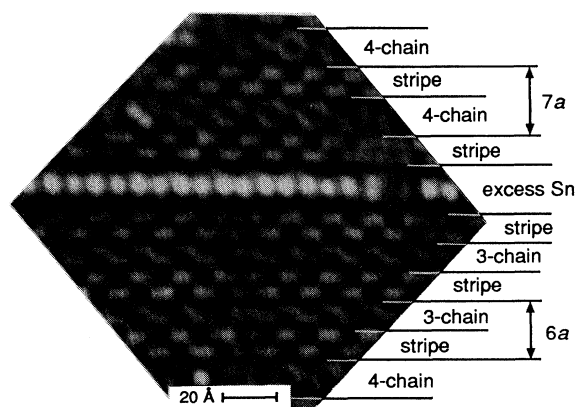


FIG. 10. Filled-state image (0.6 ML) which shows packing arrangements of the stripe structures with  $4 \times 7$  or  $4 \times 6$  local order.

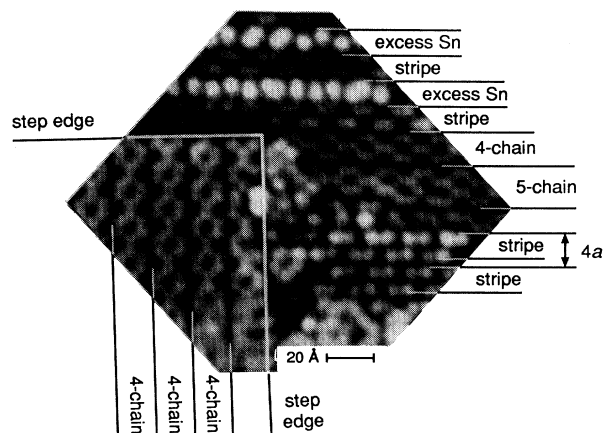


FIG. 11. Filled-state image (0.8 ML) which shows a complex arrangement of stripe, 4-chain, and 5-chain structures. Small regions with  $c(4 \times 4)$  and  $c(4 \times 8)$  local order occur.

ing are visible, where the areas between the stripes are covered by excess Sn. It is possible that the excess Sn has grown over 3-chains located between the stripes. In the lower right region of the image, there are some stripes with only a  $4a$  interstripe spacing, the minimum spacing possible. Since adjacent stripes are  $180^\circ$  out of phase, the local ordering of this small domain is  $c(4 \times 4)$ . This type of reconstruction occurs infrequently on the sample. Previous LEED studies have observed a  $c(4 \times 4)$  reconstruction at 0.375 ML, which may correspond to this collapsed stripe arrangement. Finally, in the lower left corner of the image, there are a few 4-chains with  $c(4 \times 8)$  order. The  $90^\circ$  rotation of these 4-chains with respect to the chains on the right half of the image indicates that they must be one layer above the rest of the surface (the orientation of dimer rows rotates by  $90^\circ$  across a single-height step). Since the image has been high-pass filtered to emphasize the structures on both levels, the 4-chains of the upper layer do not appear significantly brighter than those of the lower layer.

Figure 12 shows two packing arrangements of the stripes which were encountered in Figs. 10 and 11. This illustration contains three horizontal stripes, where the empty and filled states of the stripes are diagrammed as in Fig. 6. The top and middle stripes have a  $6a$  interstripe spacing and are separated by a 3-chain structure. This local  $4 \times 6$  ordering was seen in the lower half of Fig. 10. The middle and bottom stripes have the minimum  $4a$  interstripe spacing. Since it is known that the stripes are  $3a$  wide, a one unit-cell separation must exist between these stripes. This local  $c(4 \times 4)$  ordering was observed in the lower right region of Fig. 11.

The composition of the surface in terms of stripes and chains is not a straightforward matter. In addition to the behaviors observed in Figs. 10 and 11, we have also observed disordered arrangements of 4- and 5-chains on the surface with few stripes in the 0.5–0.8-ML coverage regime. There is no clear relationship between the coverage history or annealing treatment and the resulting sur-

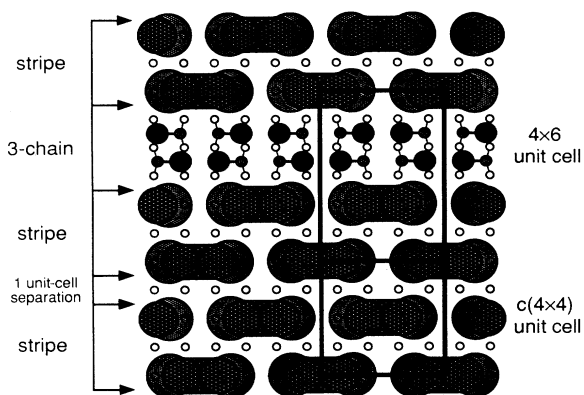


FIG. 12. Line drawing of three horizontal stripes (see Fig. 6) with appropriate spacings for  $c(4 \times 4)$  and  $4 \times 6$  local order.

face structure. Near 1 ML, however, the surface forms a global  $c(4 \times 8)$  phase consisting of 4-chains, regardless of the sample history at lower coverage. The coverage evolution up to 1 ML essentially progresses as follows: (1) development of an array of trenches, (2) formation of stripes with various structures between them [ $4 \times 14$  (4-chain between),  $4 \times 6$  (3-chain between), and  $c(4 \times 4)$  (maximum packing)], and (3) growth of chains, where the 4-chains dominate at 1 ML [ $c(4 \times 8)$ ].

#### D. Sn-Sn versus Sn-Si dimers

Up to this point, we have not addressed the possibility that Sn-Si dimers (rather than Sn-Sn dimers) could be involved in the formation of the chain structures. Since the 3-chains typically occur between stripes at lower Sn coverages, it might be possible that each buckled dimer could be a Sn-Si dimer, rather than a Sn-Sn dimer. It is difficult to distinguish between these two possibilities using STM topographs. At higher coverages near 1 ML where primarily 4- and 5-chains occur, it is reasonable to assume that primarily Sn-Sn dimers exist as a result of coverage arguments. In the case of the  $c(4 \times 8)$  reconstruction, the formation of one Sn layer of 4-chains yields a theoretical coverage of 0.75 ML Sn, consistent with the LEED values of between 0.5 and 1 ML. If the 4-chains were not composed of primarily Sn-Sn dimers, then the theoretical coverage would be much lower and not consistent with LEED. Analogous coverage arguments for the 3-chains in the  $4 \times 6$  reconstruction (Fig. 12) do not support the presence of Sn-Sn dimers. In fact, if we assume that the  $4 \times 6$  structure is complete at 0.5 ML and that the subunits of the stripe consist of four Sn atoms, then the resultant Sn density along the 3-chain requires Sn-Si dimers. Most likely, there is a gradual conversion of the buckled dimers from primarily Sn-Si dimers in the 3-chains at lower Sn coverages to primarily Sn-Sn dimers in the 4- and 5-chains at higher coverages.

This gradual conversion of the surface from Si-Sn to Sn-Sn dimers between 0.5 and 1.0 ML is partially sup-

ported by the core-level photoemission results of Rich *et al.*<sup>14</sup> In this study the population of Sn in two different bonding sites is tracked with coverage. The S1 site has the Sn atom bonded to two Si atoms, which can be associated with a Sn-Sn dimer on top of Si. The S2 site has the Sn atom bonded to three Si atoms, which can be associated with Sn in a Sn-Si dimer. As the total Sn coverage increases from 0.5 to 1.0 ML, the S2-site occupancy appears to saturate near 0.3 ML for a total Sn coverage of approximately 0.8 ML. The S1-site occupancy, however, continues to increase and reaches approximately 0.7 ML for a total Sn coverage of approximately 1.0 ML. The increase in the proportion of S1- to S2-site occupancy indicates a conversion from Sn-Si to Sn-Sn surface dimers. The remaining fraction of S2 occupancy at 1.0 ML total Sn coverage might indicate subsurface bonding of Sn, perhaps in the trenches that separate the 4-chains in the  $c(4 \times 8)$  phase.

The surface structures formed up to 1 ML coverage have been described in this section in terms of Sn substitution for Si surface atoms. This substitutional behavior raises the issue of where the displaced Si goes. Experiments involving the annealed In:Si(100) surface have demonstrated that Si displaced by surface reconstruction is mobile enough to form monolayer islands spaced hundreds of angstroms apart at annealing temperatures as low as 150 °C.<sup>5</sup> Since the annealing temperature used to form the Sn reconstructions is much higher, it is plausible that the displaced Si could migrate to step edges. The net effect would be for the displaced Si to effectively disappear at low Sn coverages. At higher coverages, however, there should be enough migrating Si to cause a significant redistribution of the surface steps. The  $c(4 \times 8)$  surface does in fact show islands on the surface, unlike the clean surface, which generally has only monotonic series of steps that reflect the local tilt of the surface. The surface is still entirely terminated by the  $c(4 \times 8)$  structure, demonstrating that the Sn has a tendency to float on the surface regardless of the rearrangement of the underlying Si.

#### IV. ANNEALED BEHAVIOR BETWEEN 1.0 AND 1.5 ML: $1 \times 5$ RECONSTRUCTION

After 1 ML Sn has been deposited and annealed, the  $c(4 \times 8)$  reconstruction completely covers the surface. Higher depositions of Sn result in the growth of bright features over the  $c(4 \times 8)$  phase. These overlayer features are visible in Fig. 13(a) after the deposition and annealing of nominally 1.2 ML Sn. Figures 13(b) and 13(c) are higher-magnification, filled-state images of surfaces with similar coverages. The new overlayer consists of bright, circular features with lateral dimensions of approximately  $1.5a$ . As the coverage is increased, the number of overlayer features increases until the surface resembles Fig. 13(d). The features are arranged into rows which are roughly  $5a$  apart, separated by trenches. Each  $1 \times 5$  row usually consists of two bright features which are spaced  $1a$  or  $2a$  apart along the length of the row. Typically, one-third of these features are displaced inward toward the center of the row [ $A$  in Fig. 13(d)], one-third are dis-

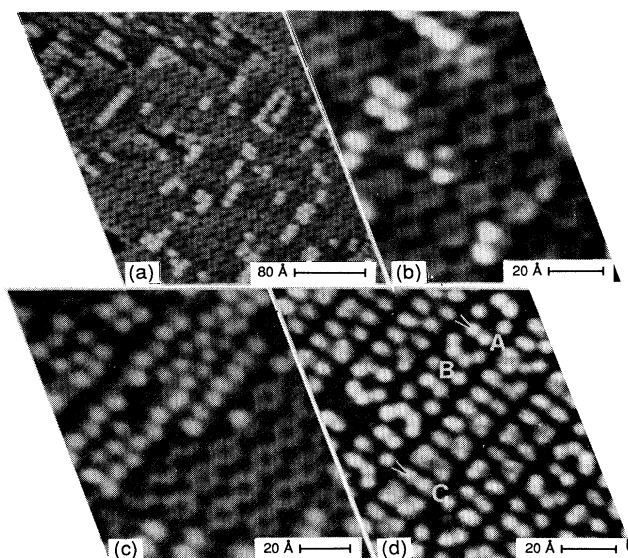


FIG. 13. Four filled-state images showing the growth of the  $1 \times 5$  phase over the  $c(4 \times 8)$  phase. As the coverage is increased above 1 ML, the number of bright overlayer features increases until the  $1 \times 5$  phase is complete at 1.5 ML [(d)].

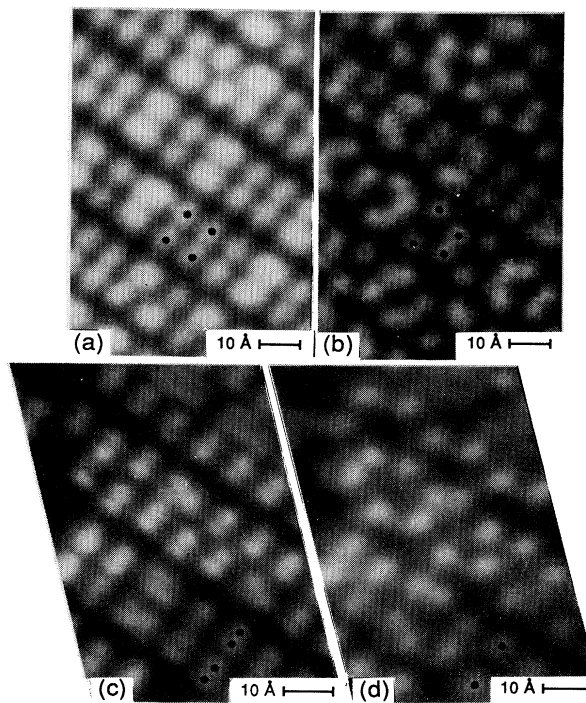


FIG. 14. Two sets of dual-bias images, showing the (a),(c) empty and (b),(d) filled states of the  $1 \times 5$  phase. The empty-state features appear uniform and consist of two overlapping maxima [(c)]. The corresponding filled-state features oftentimes appear buckled and have only one maximum [(b)].

placed outwards [ $B$  in Fig. 13(d)], and the remaining third are undisplaced and somewhat elongated [ $C$  in Fig. 13(d)]. The random positions of these features prevent the development of any global periodicity along the direction of the rows. Therefore, the only global ordering is the  $5a$  periodicity perpendicular to the rows. This surface arrangement is consistent with the  $1 \times 5$  reconstruction observed by LEED for 1–1.5 ML Sn.

Figure 14 shows dual-bias images of the empty [Figs. 14(a) and 14(c)] and filled [Figs. 14(b) and 14(d)] electronic states of the  $1 \times 5$  phase. The trenches which separate the  $1 \times 5$  rows are visible in both biases. In the first dual-bias image [Figs. 14(a) and 14(b)], two empty-state maxima typically appear relatively well aligned between the trenches [dots in Fig. 14(a)]. These two empty-state maxima correspond to two filled-state maxima, which can be displaced inward or outward toward the center of the  $1 \times 5$  row [dots in Fig. 14(b)]. In the second dual-bias image [Figs. 14(c) and 14(d)], the empty states are slightly more resolved, at the expense of the filled-state resolution. Each empty-state maximum is now actually seen to consist of two overlapping maxima. Two pairs of these maxima and their corresponding filled-state maxima are marked. Thus we find that the most fundamental unit of the  $1 \times 5$  structure corresponds to a pair of “unbuckled” maxima in the empty states and one maximum in the filled states which can be “buckled.”

The registration and approximate spatial extent of the empty and filled electronic states of the  $1 \times 5$  overlayer features are illustrated in Fig. 15. This figure contains two horizontal  $1 \times 5$  rows which are each  $5a$  wide. The top (bottom)  $1 \times 5$  row consists of bright overlayer features that are primarily unbuckled (buckled). The filled-state maxima of the bright features are represented by solid circles. The paired empty-state maxima are illustrated using two smaller gray circles which are adjacent

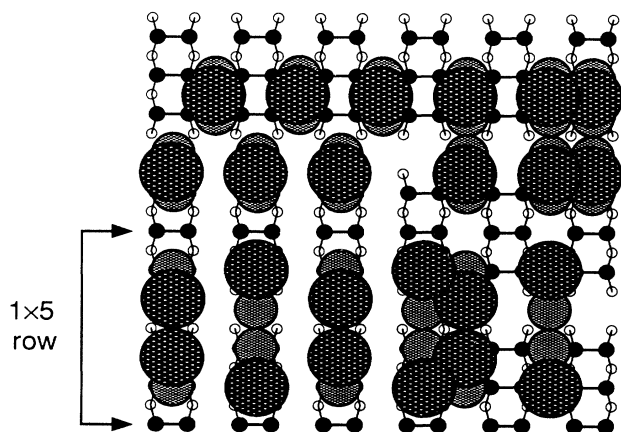


FIG. 15. Line drawing showing the filled-state (dark circles) and empty-state (paired gray circles) maxima of the  $1 \times 5$  phase. The top (bottom)  $1 \times 5$  row consists of bright overlayer features that are primarily unbuckled (buckled).

to each other. The filled-state maxima are positioned over the paired empty-state maxima according to typical configurations which occur [Fig. 13(d)]. The underlying surface is shown as an array of symmetric Sn dimers which is an approximation of an unbuckled  $c(4 \times 8)$  structure. However, we are not assigning a specific registration between the underlying  $c(4 \times 8)$  structure and the overlayer  $1 \times 5$  structure.

It should be noted that all of the maxima in the empty states are paired, and each of the maxima lies in a bridge site between two dangling bonds in the underlying layer. Thus it is highly likely that the empty-state image shows the positions of Sn-Sn dimers. Since the positions of the filled-state maxima all lie either in the center or at the end of a pair of maxima in the empty states, they are consistent with a mixture of symmetric and buckled dimers. Coverage calculations are also consistent with the formation of dimers for the  $1 \times 5$  phase. If two atoms are associated with each filled-state maximum, as expected for a dimer configuration, then typical coverage calculations from the STM images give a value of approximately 0.43 ML for the new  $1 \times 5$  overlayer. Given that the underlying surface layer is derived from a complete  $c(4 \times 8)$  phase at 1.0 ML, the resultant total coverage of 1.43 ML for the  $1 \times 5$  phase is consistent with previous LEED values.

The  $1 \times 5$  phase can thus be viewed as a half-complete layer of Sn dimers dispersed over a full monolayer of Sn. Assuming that the underlying Sn layer is still dimerized, the additional  $\sim 0.5$  ML of dimers has the effect of halving the number of surface dangling bonds. The resultant

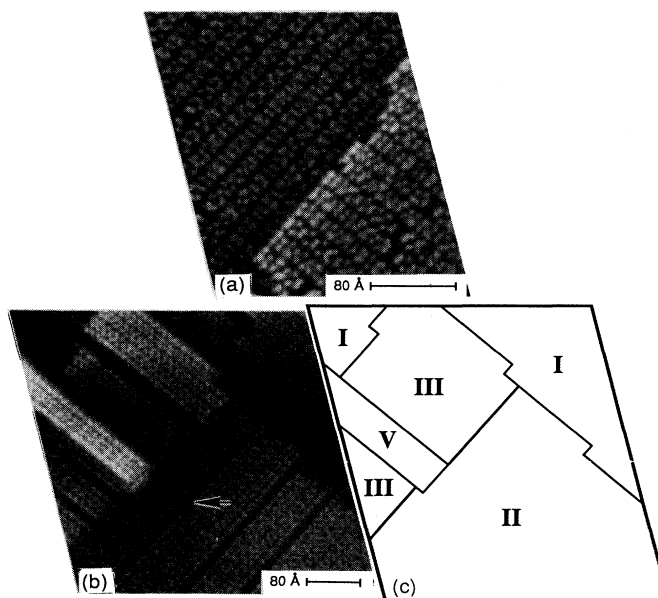


FIG. 16. Two filled-state images of the  $1 \times 5$  phase at nominally (a) 1.5 ML [(250 Å)  $\times$  (300 Å)] and (b) 1.7 ML [(450 Å)  $\times$  (480 Å)]. A line drawing [(c)] clarifies the relative heights of the  $1 \times 5$  islands in (b).

reduction in the surface energy may be a reason for the stability of the  $1 \times 5$  phase, even under additional metal deposition. A similar argument has been suggested to explain the stability of a  $\frac{4}{3}$ -ML adatom-terminated layer for Sn on GaAs(110). In this case, a  $\frac{1}{3}$ -ML layer of adatoms reduces the number of dangling bonds in the 1-ML underlayer by a factor of 3.<sup>15</sup>

Once the  $1 \times 5$  phase entirely covers the surface, additional Sn deposition initially results in layer-by-layer growth with the surface always terminated by the  $1 \times 5$  phase. Figure 16(a) shows the surface after the first  $1 \times 5$  layer is complete at 1.5 ML Sn. Figure 16(b) is a large-scale ( $\sim 460 \times 460 \text{ \AA}^2$ ) image of the surface with 1.7 ML Sn deposited and annealed. The most visible change with the additional coverage is the formation of islands at step edges. A line drawing of Fig. 16(b) is shown in Fig. 16(c) to clarify the relative heights of the islands. The original  $1 \times 5$  surface layers are labeled I and II, where the boundary between them indicates a single-height step edge. The levels corresponding to additional island growth are labeled III and V. The newly formed islands are readily identified since they have a double-height step on at least one border. Double-height steps are not observed on either the  $1 \times 5$  or  $c(4 \times 8)$  surfaces formed on the nominally flat Si(100) substrates used in this study.

It is not likely that these islands grow directly on the  $1 \times 5$  surface structure because of its sparse nature. Since the islands appear to be a means of accommodating additional Sn, it is possible that the new islands consist of two complete layers of Sn on the Si substrate, terminated by an additional 0.5 ML, which forms the  $1 \times 5$ . Presumably, the underlying Sn layers are pseudomorphic to the Si. The lower of the two Sn layers would correspond to the metal originally in the  $c(4 \times 8)$  structure. Unfortunately, it is not possible to detect any difference between the new islands and the original  $1 \times 5$  surface regions from either their appearance in the images or their single atomic step height. In principle, spectroscopic data or distance-dependent tunneling measurements might detect this difference.<sup>16</sup> These types of measurements were not attempted.

In addition to islanding, wide dark lines also appear on the surface [Fig. 16(b), arrow]. These dark lines typically interrupt the  $1 \times 5$  sequence as follows:  $1 \times 5$  row,  $3a$  wide dark trench,  $3a$  wide "half"  $1 \times 5$  row,  $1 \times 5$  row. This disruption of the  $1 \times 5$  rows could be caused by additional surface stress induced by the island growth.

#### V. ANNEALED BEHAVIOR ABOVE 2 ML: FACETING

Another 1 ML of Sn was deposited and annealed on the surface shown in Fig. 16(b) to investigate whether  $1 \times 5$  islands continued to grow [Figs. 17(a) and 17(b), near 2.5 ML]. Figure 17(a) is a  $325 \times 325 \text{ \AA}^2$  image of the surface which reveals a surprising development. Rather than the expected  $1 \times 5$  rows, only a handful of much wider rows oriented along  $\langle 011 \rangle$  directions (parallel to the original Si-dimer-row directions) are present. Figure 17(b) illustrates four very short segments of faceted rows which form a "pit" in the surface. A feature approxi-

mately  $30 \text{ \AA}$  on a side is located at the bottom of this pit. There is the possibility that this feature is contamination on the surface, but more likely it is a tip artifact caused by the finite tip radius.

These rows are typically  $15\text{--}25 \text{ \AA}$  high and are spaced  $50\text{--}80 \text{ \AA}$  apart. They have a triangular cross section with sidewalls sloped at  $\theta = 28^\circ \pm 4^\circ$  from the surface normal. A simple volume calculation of the rows ( $5 \times 10^{23}$  atoms/cm<sup>2</sup>) indicates that it is not possible for them to be formed by the three-dimensional (3D) growth of Sn ( $2 \text{ ML} = 2 \times 6.78 \times 10^{14}$  atoms/cm<sup>2</sup>). These features must then be caused by faceting of the Si(100) surface itself. Using LEED, we measured the angle between the specular reflections of the (100) surface and the facets and obtained a more precise value of  $\theta = 25.3^\circ \pm 1^\circ$ . This value indicates  $\{311\}$  planes, which intersect the (100) surface plane along  $\langle 011 \rangle$  axes and have an angle of  $25.2^\circ$  to the surface normal. Upon closer inspection of Figs. 17(a) and 17(b), closely spaced stepped terraces can be observed along the facets. These terraces have been enhanced using image processing, since the large topographic height of the facets would normally obscure such fine structure. When projected in the (100) plane, these terraces have a width separation of  $x = 5.6 \pm 0.3 \text{ \AA}$ . The  $\{311\}$  facet plane has a projected width for the  $1 \times 1$  unit cell in the (100) plane of  $x = 5.76 \text{ \AA}$ , consistent with our experimental value.

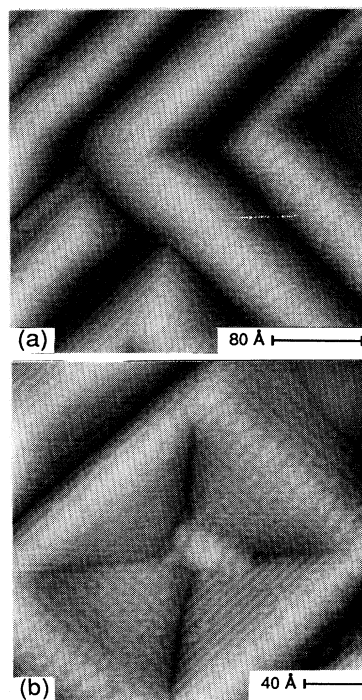


FIG. 17. Two filled-state images (a)  $325 \times 325 \text{ \AA}^2$  and (b)  $230 \times 230 \text{ \AA}^2$  of the surface with 2.5 ML Sn deposited and annealed. A gross surface rearrangement has exposed  $\{311\}$  facets.

{311} facets have also been observed in other group-IV-metal-on-Si(100) systems. In the Ge:Si(100) system, macroscopic Ge clusters with {311} facets form above 3 ML for samples annealed to 600 °C.<sup>17,18</sup> The faceting behavior of the Si(100) surface in the presence of carbon contamination is another related system.<sup>19</sup> When the Si(100) surface is contaminated with 4% carbon and annealed to 1150 °C, the carbon induces a gross surface rearrangement that exposes {311} facets. {311}-facet planes have been reported as a dominant "habit" plane of diamond-structure crystals such as Si.<sup>17</sup>

The growth of these facets may represent a final equilibrium state [e.g., macroscopic clusters for Ge:Si(100)], or a "growth-form" mechanism dominated by kinetics [e.g., facets for C:Si(100)]. Presently, we do not have sufficient information to determine the faceting mechanism. It is possible that the surface free energy is lowered by the substitution of Sn into the first few layers of the {311}-facet planes versus incorporation of Sn into the original Si(100) surface. Normally, the clean Si(311) surface has a  $3 \times 2$  reconstruction, with the  $3 \times$  periodicity oriented along the  $\langle 011 \rangle$  axis, i.e., parallel to the edge of a faceted row.<sup>20,21</sup> The component of the  $2 \times$  periodicity which is perpendicular to the  $\langle 011 \rangle$  axis has a projection onto the (100) plane equal to  $3/\sqrt{2}a_0 = 11.5$  Å. This value corresponds to the spacing between terraces on the facets and is approximately double the value seen in our STM images. This result implies that the {311} facets observed for the Sn:Si(100) system are unreconstructed. It would be interesting to grow Sn directly on the Si(311) surface in order to verify that the resulting surface is unreconstructed and to determine whether layer-by-layer growth occurs. This type of pseudomorphic growth of Sn is not observed on either Si(100) or Si(111).

## VI. CONCLUSION

We have studied both the room-temperature and annealed growth of Sn on the Si(100) surface. At room tem-

perature ( $T < 150$  °C), low coverages of Sn form rows that are oriented perpendicular to the underlying Si dimer rows. As the coverage is increased, the spacings between these rows decrease until small regions of  $2 \times 2$  form near 0.5 ML. These rows are believed to consist of dimers, as previously proposed for rows formed by group-III metals on the Si(100) surface. Previous models for these metal dimer rows assume that the metal dimer bond is oriented perpendicular to the underlying Si dimer bonds. We believe that the metal dimer bond could in fact be oriented parallel to the underlying Si dimer bonds.

For substrates annealed above 500 °C, Sn forms numerous surface structures, including trenches, stripes, chains, and bright  $1 \times 5$  overlayer features. Up to 1 ML, the surface typically evolves as follows: (1) development of an array of trenches, (2) formation of stripes with various structures between them [ $4 \times 14$  (4-chain between),  $4 \times 6$  (3-chain between), and  $c(4 \times 4)$  (maximum packing)], and (3) growth of chains, where the 4-chains dominate at 1 ML [ $c(4 \times 8)$ ]. Above 1 ML we observe the growth of bright overlayer features on the  $c(4 \times 8)$  phase, evolving into the  $1 \times 5$  phase near 1.5 ML. In spite of the complexity of these structures, we believe that many of them can be simply modeled using Sn-Si or Sn-Sn dimers. As a result, the local bonding coordination of the surface atoms is similar to that of clean Si(100). However, the Sn growth cannot be described as pseudomorphic. The size difference between the Sn and Si atoms has a strong effect on the long-range order of the surface with the resultant formation of various reconstructions. Above approximately 2 ML, the surface undergoes a gross rearrangement and forms {311} facets.

## ACKNOWLEDGMENTS

This research was performed at Stanford University and supported by the Office of Naval Research. One of the authors (A.A.B.) acknowledges support received from AT&T.

<sup>1</sup>S. Park and C. F. Quate, Rev. Sci. Instrum. **58**, 2010 (1987).

<sup>2</sup>Commercial STM provided by Park Scientific Instruments, Inc., Sunnyvale, CA 94089.

<sup>3</sup>J. Nogami, A. A. Baski, and C. F. Quate, Phys. Rev. B **44**, 1415 (1991).

<sup>4</sup>A. A. Baski, J. Nogami, and C. F. Quate, J. Vac. Sci. Technol. A **8**, 245 (1990).

<sup>5</sup>A. A. Baski, J. Nogami, and C. F. Quate, J. Vac. Sci. Technol. A **9**, 1946 (1991).

<sup>6</sup>T. Ide, T. Nishimori, and T. Ichinokawa, Surf. Sci. **209**, 335 (1989).

<sup>7</sup>B. Bourguignon, K. L. Carleton, and S. R. Leone, Surf. Sci. **204**, 455 (1988).

<sup>8</sup>D. H. Rich, A. Samsavar, T. Miller, H. F. Lin, and T.-C. Chiang, Phys. Rev. Lett. **58**, 579 (1987).

<sup>9</sup>Y.-W. Mo, R. Kariotis, B. S. Swartzentruber, M. B. Webb, and M. G. Lagally, J. Vac. Sci. Technol. A **8**, 201 (1990).

<sup>10</sup>J. Knall, J.-E. Sundgren, G. V. Hansson, and J. E. Greene, Surf. Sci. **166**, 512 (1986).

<sup>11</sup>J. E. Northrup, Phys. Rev. Lett. **57**, 154 (1986).

<sup>12</sup>K. Ueda, K. Kinoshita, and M. Mannami, Surf. Sci. **145**, 261 (1984).

<sup>13</sup>O. L. Alerhand, D. Vanderbilt, R. D. Meade, and J. D. Joannopoulos, Phys. Rev. Lett. **61**, 1973 (1988).

<sup>14</sup>D. H. Rich, T. Miller, A. Samsavar, H. F. Lin, and T.-C. Chiang, Phys. Rev. B **37**, 10221 (1988).

<sup>15</sup>C. K. Shih, E. Kaxiras, R. M. Feenstra, and K. C. Pandey, Phys. Rev. B **40**, 10044 (1989).

<sup>16</sup>J. A. Kubby, Y. R. Wang, and W. J. Greene, Phys. Rev. Lett. **65**, 2165 (1990).

<sup>17</sup>Y. Koide, S. Zaima, N. Ohshima, and Y. Yasuda, Jpn. J. Appl. Phys. **28**, 690 (1989).

<sup>18</sup>Y.-W. Mo, D. E. Savage, B. S. Swartzentruber, and M. G. Lagally, Phys. Rev. Lett. **65**, 1020 (1990).

<sup>19</sup>Y. Yang and E. D. Williams, J. Vac. Sci. Technol. A **8**, 2481 (1990).

<sup>20</sup>J. Knall, J. B. Pethica, J. D. Todd, and J. H. Wilson, Phys. Rev. Lett. **66**, 1733 (1991).

<sup>21</sup>U. Myler and K. Jacobi, Surf. Sci. **220**, 353 (1989).

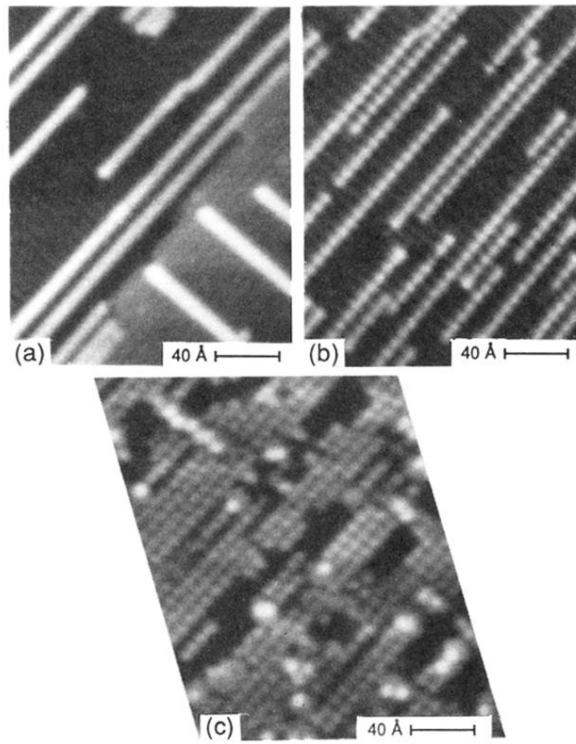


FIG. 1. Three images with (a) 0.1, (b) 0.15, and (c) 0.5 ML Sn deposited near room temperature. Both empty-electronic-state [(a) and (b)] and filled-state [(c)] images are shown. Bright Sn dimer rows are oriented perpendicular to the underlying Si dimer rows.

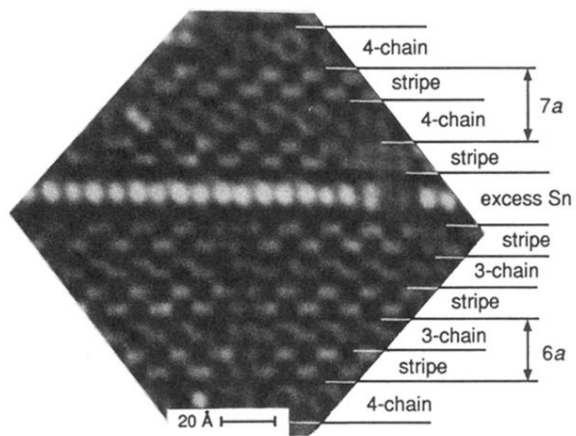


FIG. 10. Filled-state image (0.6 ML) which shows packing arrangements of the stripe structures with  $4 \times 7$  or  $4 \times 6$  local order.

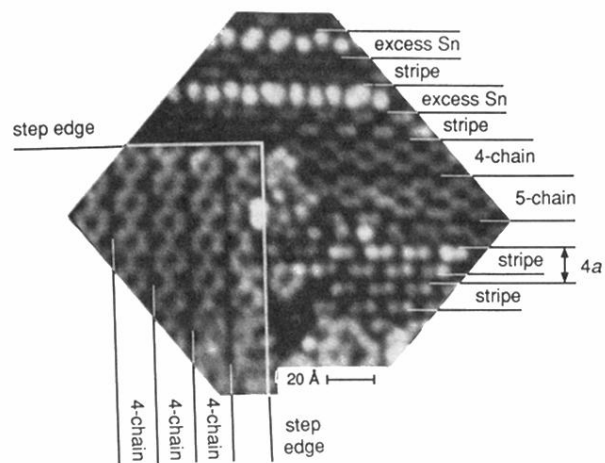


FIG. 11. Filled-state image (0.8 ML) which shows a complex arrangement of stripe, 4-chain, and 5-chain structures. Small regions with  $c(4 \times 4)$  and  $c(4 \times 8)$  local order occur.

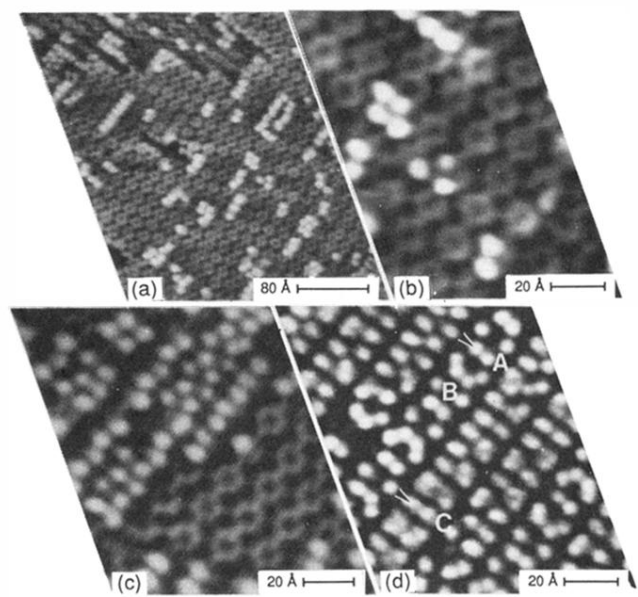


FIG. 13. Four filled-state images showing the growth of the  $1 \times 5$  phase over the  $c(4 \times 8)$  phase. As the coverage is increased above 1 ML, the number of bright overlayer features increases until the  $1 \times 5$  phase is complete at 1.5 ML [(d)].

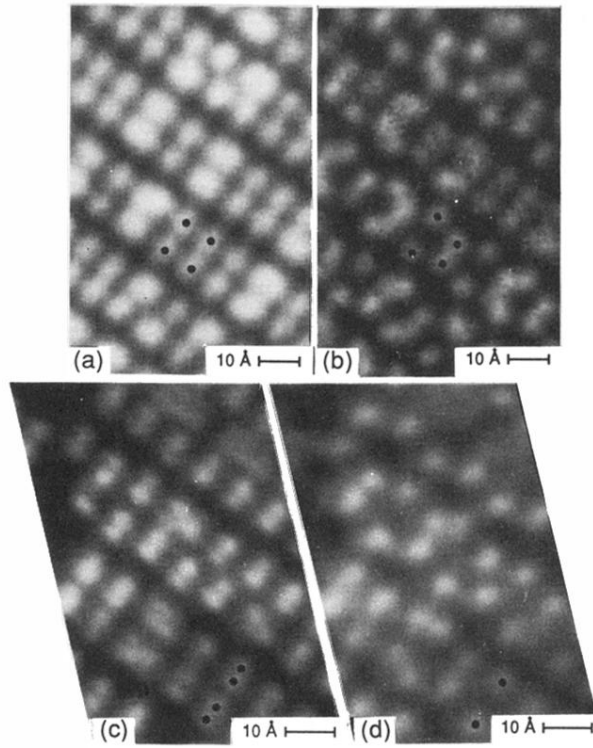


FIG. 14. Two sets of dual-bias images, showing the (a),(c) empty and (b),(d) filled states of the  $1 \times 5$  phase. The empty-state features appear uniform and consist of two overlapping maxima [(c)]. The corresponding filled-state features oftentimes appear buckled and have only one maximum [(b)].

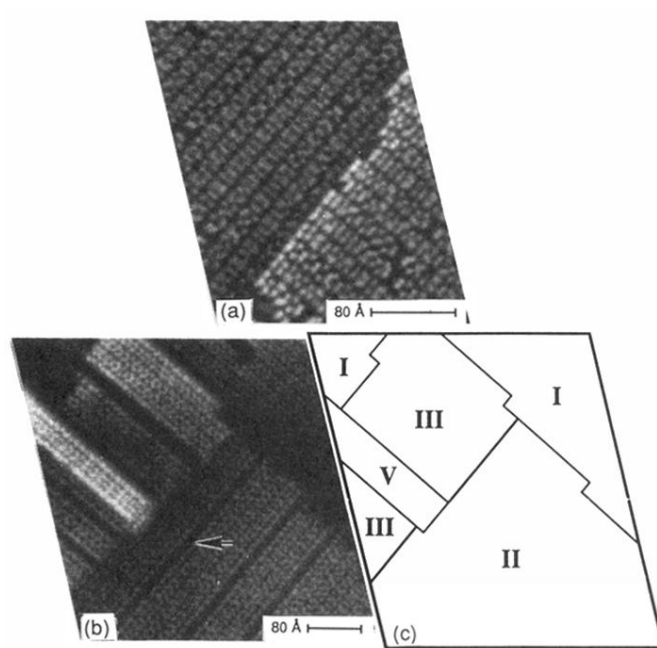


FIG. 16. Two filled-state images of the  $1 \times 5$  phase at nominally (a) 1.5 ML [(250 Å)  $\times$  (300 Å)] and (b) 1.7 ML [(450 Å)  $\times$  (480 Å)]. A line drawing [(c)] clarifies the relative heights of the  $1 \times 5$  islands in (b).

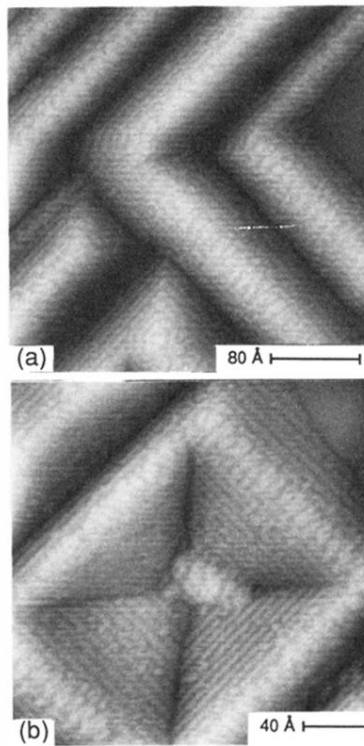


FIG. 17. Two filled-state images (a)  $325 \times 325 \text{ \AA}^2$  and (b)  $230 \times 230 \text{ \AA}^2$  of the surface with 2.5 ML Sn deposited and annealed. A gross surface rearrangement has exposed  $\{311\}$  facets.

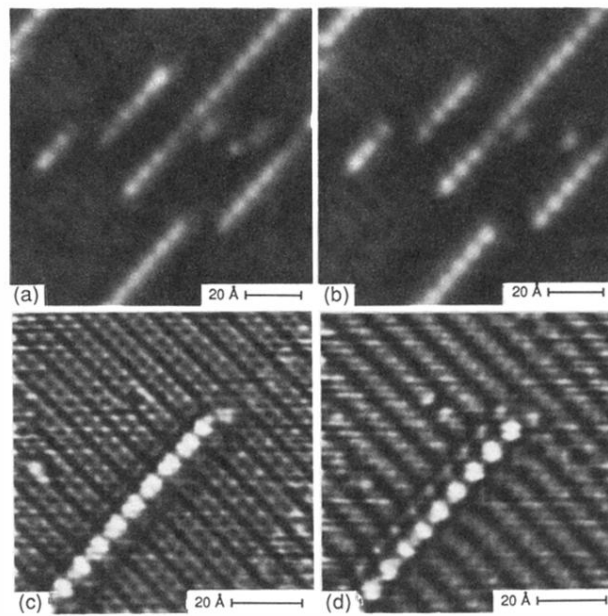


FIG. 2. (a), (b) Dual-bias topograph showing the (a) empty and (b) filled states of the Sn dimer rows. (c), (d) Dual-bias image showing the local curvature of the surface for the (c) empty and (d) filled states. The maxima along the Sn dimer rows are located in the troughs between the underlying Si dimer rows.

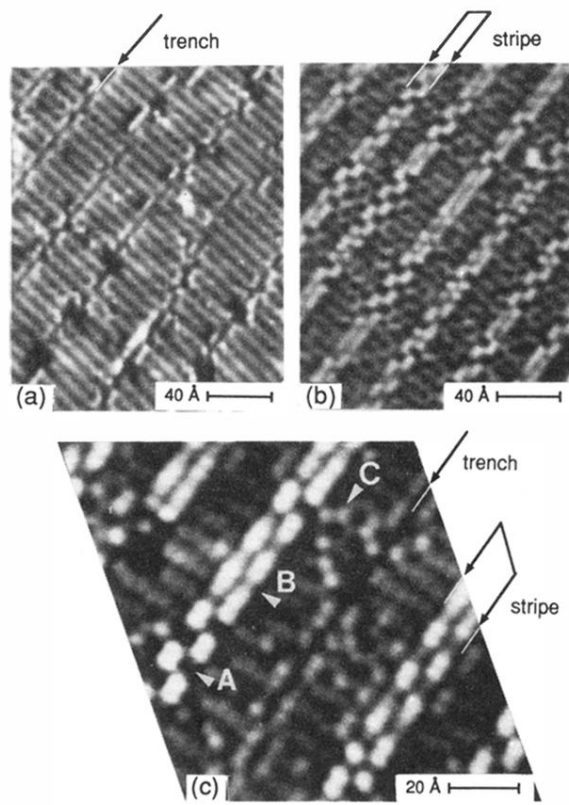


FIG. 4. Three filled-state images with nominally (a) 0.2, (b) 0.4, and (c) 0.4 ML Sn deposited and annealed. Both the trench and stripe structures are indicated.

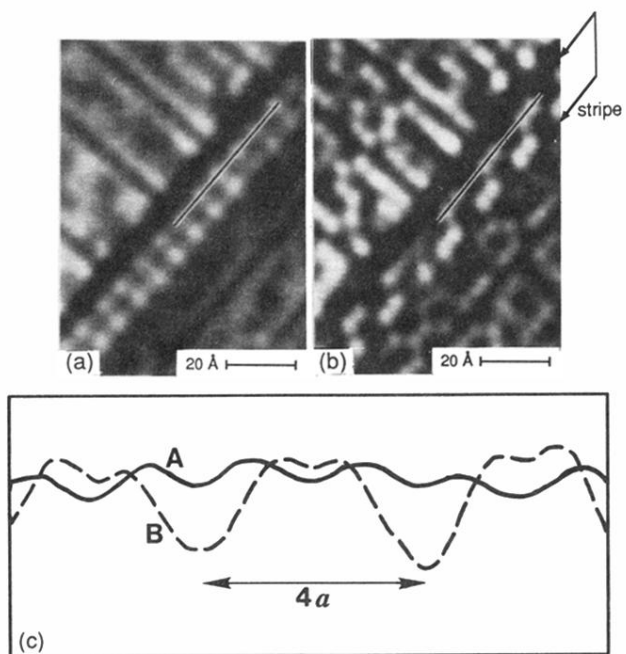


FIG. 5. Dual-bias image of a stripe showing the (a) empty and (b) filled states. The bottom line drawing [(c)] is a cross-sectional trace along the indicated left side of the stripe.

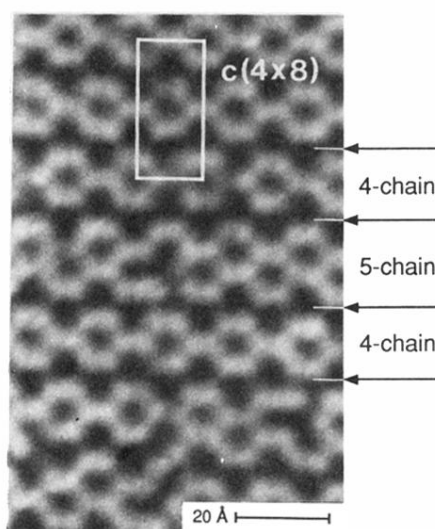


FIG. 7. Filled-state image (0.8 ML) showing the 4- and 5-chain structures. A  $c(4 \times 8)$  unit cell is indicated.

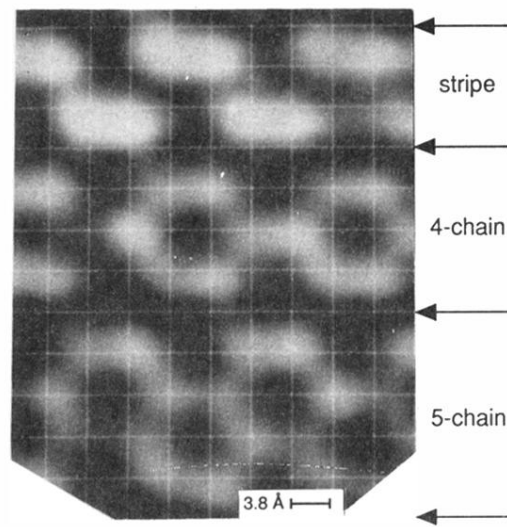


FIG. 8. Filled-state image with a superimposed  $1 \times 1$  unit-cell grid, which explicitly shows the widths of a stripe, 4-chain, and 5-chain.